optic nerve was immediately placed into a fixative consisting of 2.5% glutaraldehyde and 2% formaldehyde in 0.1 M cacodylate buffer with 0.08 M $CaCl_2$ overnight at 4 °C. The tissue was then washed in 0.1 M cacodylate buffer and postfixed in 2% aqueous $OsO_4$. The segments were dehydrated in graded alcohols and embedded in epon. One-micrometer sections were cut and stained with 1% toluidine blue in 1% borate buffer. The photomicrographs used for axon counting were taken at 5 fixed positions (center, superior, inferior, nasal and temporal) with an ×100 objective on a microscope (DMRXA, Leica). Axon counting was carried out in a masked fashion as previously described (Nakazawa et al., 2006).

### 4.5. *Immunohistochemistry*

Immunohistochemistry (IHC) was performed as previously described (Nakazawa et al., 2006, 2007a). Briefly, the eyes were surgically removed with the optic nerve still attached and fixed with 4% PFA overnight at 4 °C, and then cryoprotected with PBS containing 20% sucrose. Cryo-sections (thickness 10 μm) of the retina and optic nerve were mounted on the slides and incubated with blocking buffer (10% goat serum, 0.5% gelatin, 3% bovine serum albumin (BSA) and 0.2% Tween 20 in PBS). Next, they were incubated with rabbit anti-ApoE antibody (Biodesign, K23100R, 1:400), mouse anti-phosphorylated neurofilaments as a marker of surviving axons (Convance, SMI-31R, 1:500), mouse anti-glutamine synthetase as a marker of Müller cells (Chemicon, MAB302, 1:200), or mouse anti-GFAP as a marker of astrocytes (Simga, G3893, 1:200) overnight at 4 °C. Blocking buffers without primary antibodies served as negative controls. The sections were washed three times with PBST (PBS containing 0.2% Tween 20) and then incubated with an Alexa 488 or Alexa 568 secondary antibody (1:200, Invitrogen) for 1 h. The slides were washed three times and mounted with the VECTASHIELD Mounting Medium with DAPI (H-1200, Vector Laboratories, Burlingame, CA).

### 4.6. *Statistical analysis*

The data were analyzed with ANOVA followed by Scheffe's post-hoc test or Mann–Whitney *U*-tests with the software "EXCEL statistics" (SSRI, Tokyo, Japan). A $p$ value $<0.05$ was considered statistically significant and is highlighted in all figures with an asterisk. All values are expressed as the mean ± standard deviation (SD).

## Acknowledgments

No authors have any financial disclosures. The authors thank Mr. Tim Hilts for editing this manuscript. This paper was supported in part by JSPS KAKENHI Grants-in-Aid for Scientific Research (B) (T.N. 26293372), (C) (K.M. 26462677), and for Exploratory Research (T.N. 26670751, Y.T. 26670263).

## REFERENCES

Amaratunga, A., Abraham, C.R., Edwards, R.B., Sandell, J.H., Schreiber, B.M., Fine, R.E., 1996. Apolipoprotein E is synthesized in the retina by Muller glial cells, secreted into the vitreous, and rapidly transported into the optic nerve by retinal ganglion cells. J. Biol. Chem. 271, 5628–5632.

Boyles, J.K., Pitas, R.E., Wilson, E., Mahley, R.W., Taylor, J.M., 1985. Apolipoprotein E associated with astrocytic glia of the central nervous system and with nonmyelinating glia of the peripheral nervous system. J. Clin. Invest. 76, 1501–1513.

Bu, G., 2009. Apolipoprotein E and its receptors in Alzheimer's disease: pathways, pathogenesis and therapy. Nat. Rev. Neurosci. 10, 333–344.

Collaborative Normal-Tension Glaucoma Study Group, 1998. The effectiveness of intraocular pressure reduction in the treatment of normal-tension glaucoma. Am. J. Ophthalmol. 126, 498–505.

De Castro, D.K., Punjabi, O.S., Bostrom, A.G., Stamper, R.L., Lietman, T.M., Ray, K., Lin, S.C., 2007. Effect of statin drugs and aspirin on progression in open-angle glaucoma suspects using confocal scanning laser ophthalmoscopy. Clin. Exp. Ophthalmol. 35, 506–513.

Ganesh, B.S., Chintala, S.K., 2011. Inhibition of reactive gliosis attenuates excitotoxicity-mediated death of retinal ganglion cells. PLoS One 6, e18305.

Gee, J.R., Keller, J.N., 2005. Astrocytes: regulation of brain homeostasis via apolipoprotein E. Int. J. Biochem. Cell Biol. 37, 1145–1150.

Hayashi, H., Campenot, R.B., Vance, D.E., Vance, J.E., 2004. Glial lipoproteins stimulate axon growth of central nervous system neurons in compartmented cultures. J. Biol. Chem. 279, 14009–14015.

Hayashi, H., Campenot, R.B., Vance, D.E., Vance, J.E., 2007. Apolipoprotein E-containing lipoproteins protect neurons from apoptosis via a signaling pathway involving low-density lipoprotein receptor-related protein-1. J. Neurosci. 27, 1933–1941.

Hayashi, H., Campenot, R.B., Vance, D.E., Vance, J.E., 2009. Protection of neurons from apoptosis by apolipoprotein E-containing lipoproteins does not require lipoprotein uptake and involves activation of phospholipase Cgamma1 and inhibition of calcineurin. J. Biol. Chem. 284, 29605–29613.

Hayashi, H., Eguchi, Y., Fukuchi-Nakaishi, Y., Takeya, M., Nakagata, N., Tanaka, K., Vance, J.E., Tanihara, H., 2012. A potential neuroprotective role of apolipoprotein E-containing lipoproteins through low density lipoprotein receptor-related protein 1 in normal tension glaucoma. J. Biol. Chem. 287, 25395–25406.

Heijl, A., Leske, M.C., Bengtsson, B., Hyman, L., Hussein, M., 2002. Reduction of intraocular pressure and glaucoma progression: results from the Early Manifest Glaucoma Trial. Arch. Ophthalmol. 120, 1268–1279.

Himori, N., Yamamoto, K., Maruyama, K., Ryu, M., Taguchi, K., Yamamoto, M., Nakazawa, T., 2013. Critical role of Nrf2 in oxidative stress-induced retinal ganglion cell death. J. Neurochem. 127, 669–680.

Honjo, M., Tanihara, H., Nishijima, K., Kiryu, J., Honda, Y., Yue, B.Y., Sawamura, T., 2002. Statin inhibits leukocyte-endothelial interaction and prevents neuronal death induced by ischemia-reperfusion injury in the rat retina. Arch. Ophthalmol. 120, 1707–1713.

Ito, J.I., Nagayasu, Y., Miura, Y., Yokoyama, S., Michikawa, M., 2014. Astrocytes endogenous apoE generates HDL-like lipoproteins using previously synthesized cholesterol through interaction with ABCA1. Brain Res..

Iwase, A., Suzuki, Y., Araie, M., Yamamoto, T., Abe, H., Shirato, S., Kuwayama, Y., Mishima, H.K., Shimizu, H., Tomita, G., Inoue, Y., Kitazawa, Y., 2004. The prevalence of primary open-angle

glaucoma in Japanese: the Tajimi Study. Ophthalmology 111, 1641–1648.
Jablonski, M.M., Iannaccone, A., 2000. Targeted disruption of Muller cell metabolism induces photoreceptor dysmorphogenesis. Glia 32, 192–204.
Kashiwagi, K., Ou, B., Nakamura, S., Tanaka, Y., Suzuki, M., Tsukahara, S., 2003. Increase in dephosphorylation of the heavy neurofilament subunit in the monkey chronic glaucoma model. Invest. Ophthalmol. Vis. Sci. 44, 154–159.
Kawaji, T., Inomata, Y., Takano, A., Sagara, N., Inatani, M., Fukushima, M., Tanihara, H., Honjo, M., 2007. Pitavastatin: protection against neuronal retinal damage induced by ischemia-reperfusion injury in rats. Curr. Eye Res. 32, 991–997.
Kim, C.S., Seong, G.J., Lee, N.H., Song, K.C., 2011. Prevalence of primary open-angle glaucoma in central South Korea the Namil study. Ophthalmology 118, 1024–1030.
Kurumada, S., Onishi, A., Imai, H., Ishii, K., Kobayashi, T., Sato, S.B., 2007. Stage-specific association of apolipoprotein A-I and E in developing mouse retina. Invest. Ophthalmol. Vis. Sci. 48, 1815–1823.
Lam, C.Y., Fan, B.J., Wang, D.Y., Tam, P.O., Yung Tham, C.C., Leung, D.Y., Ping Fan, D.S., Chiu Lam, D.S., Pang, C.P., 2006. Association of apolipoprotein E polymorphisms with normal tension glaucoma in a Chinese population. J. Glaucoma. 15, 218–222.
Levin, L.A., 2003. Retinal ganglion cells and neuroprotection for glaucoma. Surv. Ophthalmol. 48 (Suppl. 1), S21–S24.
Liang, Y.B., Friedman, D.S., Zhou, Q., Yang, X., Sun, L.P., Guo, L.X., Tao, Q.S., Chang, D.S., Wang, N.L., 2011. Prevalence of primary open angle glaucoma in a rural adult Chinese population: the Handan eye study. Invest. Ophthalmol. Vis. Sci. 52, 8250–8257.
Libby, R.T., Anderson, M.G., Pang, I.H., Robinson, Z.H., Savinova, O.V., Cosma, I.M., Snow, A., Wilson, L.A., Smith, R.S., Clark, A.F., John, S.W., 2005a. Inherited glaucoma in DBA/2J mice: pertinent disease features for studying the neurodegeneration. Vis. Neurosci. 22, 637–648.
Libby, R.T., Li, Y., Savinova, O.V., Barter, J., Smith, R.S., Nickells, R.W., John, S.W., 2005b. Susceptibility to neurodegeneration in a glaucoma is modified by Bax gene dosage. PLoS Genet. 1, 17–26.
Mabuchi, F., Tang, S., Ando, D., Yamakita, M., Wang, J., Kashiwagi, K., Yamagata, Z., Iijima, H., Tsukahara, S., 2005. The apolipoprotein E gene polymorphism is associated with open angle glaucoma in the Japanese population. Mol. Vis. 11, 609–612.
Mahley, R.W., 1988. Apolipoprotein E: cholesterol transport protein with expanding role in cell biology. Science 240, 622–630.
Marcus, M.W., Muskens, R.P., Ramdas, W.D., Wolfs, R.C., De Jong, P.T., Vingerling, J.R., Hofman, A., Stricker, B.H., Jansonius, N. M., 2012. Cholesterol-lowering drugs and incident open-angle glaucoma: a population-based cohort study. PLoS One 7, e29724.
Matsubara, A., Nakazawa, T., Husain, D., Iliaki, E., Connolly, E., Michaud, N.A., Gragoudas, E.S., Miller, J.W., 2006. Investigating the effect of ciliary body photodynamic therapy in a glaucoma mouse model. Invest. Ophthalmol. Vis. Sci. 47, 2498–2507.
Morgan, J.E., 2000. Optic nerve head structure in glaucoma: astrocytes as mediators of axonal damage. Eye 14 (Pt 3B), 437–444.
Nakazawa, T., Nakazawa, C., Matsubara, A., Noda, K., Hisatomi, T., She, H., Michaud, N., Hafezi-Moghadam, A., Miller, J.W., Benowitz, L.I., 2006. Tumor necrosis factor-alpha mediates oligodendrocyte death and delayed retinal ganglion cell loss in a mouse model of glaucoma. J. Neurosci. 26, 12633–12641.
Nakazawa, T., Hisatomi, T., Nakazawa, C., Noda, K., Maruyama, K., She, H., Matsubara, A., Miyahara, S., Nakao, S., Yin, Y., Benowitz, L., Hafezi-Moghadam, A., Miller, J.W., 2007a. Monocyte chemoattractant protein 1 mediates retinal detachment-induced photoreceptor apoptosis. Proc. Natl. Acad. Sci. USA 104, 2425–2430.
Nakazawa, T., Takahashi, H., Nishijima, K., Shimura, M., Fuse, N., Tamai, M., Hafezi-Moghadam, A., Nishida, K., 2007b. Pitavastatin prevents NMDA-induced retinal ganglion cell death by suppressing leukocyte recruitment. J. Neurochem. 100, 1018–1031.
Nakazawa, T., Shimura, M., Ryu, M., Nishida, K., Pages, G., Pouyssegur, J., Endo, S., 2008. ERK1 plays a critical protective role against N-methyl-D-aspartate-induced retinal injury. J. Neurosci. Res. 86, 136–144.
Ong, J.M., Zorapapel, N.C., Rich, K.A., Wagstaff, R.E., Lambert, R.W., Rosenberg, S.E., Moghaddas, F., Pirouzmanesh, A., Aoki, A.M., Kenney, M.C., 2001. Effects of cholesterol and apolipoprotein E on retinal abnormalities in ApoE-deficient mice. Invest. Ophthalmol. Vis. Sci. 42, 1891–1900.
Ong, J.M., Zorapapel, N.C., Aoki, A.M., Brown, D.J., Nesburn, A.B., Rich, K.A., Kenney, C.M., 2003. Impaired electroretinogram (ERG) response in apolipoprotein E-deficient mice. Curr. Eye Res. 27, 15–24.
Quigley, H.A., 1996. Number of people with glaucoma worldwide. Br. J. Ophthalmol. 80, 389–393.
Resnikoff, S., Pascolini, D., Etya'ale, D., Kocur, I., Pararajasegaram, R., Pokharel, G.P., Mariotti, S.P., 2004. Global data on visual impairment in the year 2002. Bull. World Health Organ. 82, 844–851.
Ressiniotis, T., Griffiths, P.G., Birch, M., Keers, S., Chinnery, P.F., 2004. The role of apolipoprotein E gene polymorphisms in primary open-angle glaucoma. Arch. Ophthalmol. 122, 258–261.
Ryu, M., Yasuda, M., Shi, D., Shanab, A.Y., Watanabe, R., Himori, N., Omodaka, K., Yokoyama, Y., Takano, J., Saido, T., Nakazawa, T., 2012. Critical role of calpain in axonal damage-induced retinal ganglion cell death. J. Neurosci. Res. 90, 802–815.
Schmitt, U., Sabel, B.A., 1996. MK-801 reduces retinal ganglion cell survival but improves visual performance after controlled optic nerve crush. J. Neurotrauma. 13, 791–800.
Schuettauf, F., Naskar, R., Vorwerk, C.K., Zurakowski, D., Dreyer, E.B., 2000. Ganglion cell loss after optic nerve crush mediated through AMPA-kainate and NMDA receptors. Invest. Ophthalmol. Vis. Sci. 41, 4313–4316.
Shanab, A.Y., Nakazawa, T., Ryu, M., Tanaka, Y., Himori, N., Taguchi, K., Yasuda, M., Watanabe, R., Takano, J., Saido, T., Minegishi, N., Miyata, T., Abe, T., Yamamoto, M., 2012. Metabolic stress response implicated in diabetic retinopathy: the role of calpain, and the therapeutic impact of calpain inhibitor. Neurobiol. Dis. 48, 556–567.
Suzuki, Y., Iwase, A., Araie, M., Yamamoto, T., Abe, H., Shirato, S., Kuwayama, Y., Mishima, H.K., Shimizu, H., Tomita, G., Inoue, Y., Kitazawa, Y., 2006. Risk factors for open-angle glaucoma in a Japanese population: the Tajimi Study. Ophthalmology 113, 1613–1617.
Tamura, H., Kawakami, H., Kanamoto, T., Kato, T., Yokoyama, T., Sasaki, K., Izumi, Y., Matsumoto, M., Mishima, H.K., 2006. High frequency of open-angle glaucoma in Japanese patients with Alzheimer's disease. J. Neurol. Sci. 246, 79–83.
Weinreb, R.N., Khaw, P.T., 2004. Primary open-angle glaucoma. Lancet 363, 1711–1720.
Yasuda, M., Tanaka, Y., Ryu, M., Tsuda, S., Nakazawa, T., 2014. RNA sequence reveals mouse retinal transcriptome changes early after axonal injury. PLoS One 9, e93258.
Zetterberg, M., Tasa, G., Palmer, M.S., Juronen, E., Teesalu, P., Blennow, K., Zetterberg, H., 2007. Apolipoprotein E polymorphisms in patients with primary open-angle glaucoma. Am. J. Ophthalmol. 143, 1059–1060.
Zhang, X., Cheng, M., Chintala, S.K., 2004. Kainic acid-mediated upregulation of matrix metalloproteinase-9 promotes retinal degeneration. Invest. Ophthalmol. Vis. Sci. 45, 2374–2383.

Journal of Neuroscience Research

Journal of Neuroscience Research 92:1637–1646 (2014)

# Artemin Augments Survival and Axon Regeneration in Axotomized Retinal Ganglion Cells

**Kazuko Omodaka,[1] Takuji Kurimoto,[2] Orie Nakamura,[1] Kota Sato,[1] Masayuki Yasuda,[1] Yuji Tanaka,[1] Noriko Himori,[1] Yu Yokoyama,[1] and Toru Nakazawa[1,3,4]★**

[1]Department of Ophthalmology and Visual Science, Tohoku University Graduate School of Medicine, Sendai, Japan
[2]Department of Ophthalmology, Mimihara General Hospital, Sakai, Japan
[3]Department of Advanced Ophthalmic Medicine, Tohoku University Graduate School of Medicine, Sendai, Japan
[4]Department of Retinal Disease Control, Tohoku University Graduate School of Medicine, Sendai, Japan

Artemin, a recently discovered member of the glial cell line-derived neurotrophic factor (GDNF) family, has neurotrophic effects on damaged neurons, including sympathetic neurons, dopamine neurons, and spiral ganglion neurons both in vivo and in vitro. However, its effects on retinal cells and its intracellular signaling remain relatively unexplored. During development, expression of GFRα3, a specific receptor for artemin, is strong in the immature retina and gradually decreases during maturation, suggesting a possible role in the formation of retinal connections. Optic nerve damage in mature rats causes levels of GFRα3 mRNA to increase tenfold in the retina within 3 days. GFRα3 mRNA levels continue to rise within the first week and then decline. Artemin, a specific ligand for GFRα3, has a neuroprotective effect on axotomized retinal ganglion cells (RGCs) in vivo and in vitro via activation of the extracellular signal-related kinase– and phosphoinositide 3-kinase–Akt signaling pathways. Artemin also has a substantial effect on axon regeneration in RGCs both in vivo and in vitro, whereas other GDNF family members do not. Therefore, artemin/GFRα3, but not other GDNF family members, may be of value for optic nerve regeneration in mature mammals. 

**Key words:** retinal ganglion cell; regeneration; growth factor; signal transduction; mitogen-activated protein kinase; optic nerve axotomy; glaucoma

Glial cell line-derived neurotrophic factor (GDNF) was initially identified as a factor secreted from a glioma cell line that can support the survival of embryonic ventral midbrain neurons in culture (Lin et al., 1993). Subsequent studies have shown that GDNF is an important trophic factor for multiple types of neurons and glia (Baloh et al., 2000). Additional members of the GDNF family have since been identified (Lindahl et al., 2000; Carmillo et al., 2005) and include neurturin (NRTN), artemin (ARTN), and persephin (PSPN). GDNF family ligands activate the receptor tyrosine kinase Ret through binding of glycosylphosphatidylinositol-anchored GDNF family receptor α (GFRα) coreceptors 1–4 (Sariola and Saarma, 2003). GDNF binds GFRα1, NRTN binds GFRα2, ARTN binds GFRα3, and PSPN binds GFRα4 (Lindahl et al., 2000; Carmillo et al., 2005). These receptors have no kinase domain but act through the associated Ret tyrosine kinase, leading to Ret autophosphorylation and the initiation of intracellular signaling. Downstream signaling includes the activation of mitogen-activated protein kinase (MAPK), phosphoinositide 3-kinase (PI3K)–AKT, phospholipase Cγ, cAMP response element-binding (CREB), and Src-family kinases (SFK) pathways (Trupp et al., 1999; Baloh et al., 2000; Jeong et al., 2008). In addition, GFRs can potentially activate CREB directly through a Ret-independent mechanism (Trupp et al., 1999). The regulation of GFR expression would be expected to play a pivotal role in controlling ligand-mediated effects. For example, GFRα3 is highly expressed on embryonic day 11 but is not appreciably expressed in adult mouse of dorsal root ganglia (DRG) or superior cervical sympathetic ganglion (SCG; Worby et al., 1998).

Contract grant sponsor: JSPS Grants-in-Aid for Scientific Research (B), contract grant number: 26293372 (to T.N.); Contract grant sponsor: JSPS Grants-in-Aid for Exploratory Research, contract grant numbers: 26670751 (to T.N.); 26670263 (Y.T.); Contract grant sponsor: JSPS Grants-in-Aid for Young Scientists, contract grant number: 26861434 (to N.H.).

*Correspondence to: Toru Nakazawa, MD, PhD, Department of Ophthalmology, Tohoku University Graduate School of Medicine, 1-1, Seiryo, Aoba, Sendai, Miyagi 980-8574, Japan.
E-mail: ntoru@fa2.so-net.ne.jp

Received 17 April 2014; Revised 3 June 2014; Accepted 10 June 2014

**Published online 9 July 2014 in Wiley Online Library (wileyonlinelibrary.com). DOI: 10.1002/jnr.23449**

GDNF, NRTN, and PSPN exert neuroprotective effects on injured neurons through the PI3K−Akt signaling pathway. This pathway has been shown to be important in preventing the death of retinal ganglion cells (RGCs) in various pathological conditions (Nakazawa et al., 2002b, 2003, 2005b). In isolated retinal Muller glial cells, stimulation of GDNF-family protein resulted in the transcriptional upregulation of FGF-2 (Hauck et al., 2006). Although the roles of GDNF-GFRα1 and NRTN-GFRα2 have been characterized to some extent in the visual system (Hauck et al., 2006; Brantley et al., 2008; Koeberle and Bahr, 2008), the roles of ARTN and GFRα3 remain unknown.

This study examined the changes in expression of growth factor receptors after optic nerve axotomy and showed that GFRα3 receptors were selectively upregulated. We also investigated the role of GDNF-family receptor genes in retinal development, in the optic nerve following axotomy, and in retinal primary cultures. Our data suggest that GDNF-family proteins have a substantial neuroprotective effect on RGCs and that ARTN, a recently discovered member of the GDNF family, has unique effects on axon regeneration.

## MATERIALS AND METHODS

### Animals and Surgical Procedure

One hundred thirty-six male Sprague-Dawley rats (SLC, Hamamatsu, Japan) weighing 200–240 g were used in this study. All animals were maintained and handled in accordance with the ARVO Statement for the Use of Animals in Ophthalmic and Vision Research.

Transection of the optic nerve was performed on the right eye as previously described (Nakazawa et al., 2002a,b). In brief, rats were anesthetized via intraperitoneal injection of sodium pentobarbital (Nembutal; 45 mg/kg of body weight), and the optic nerve was transected about 1 mm posterior to the eyeball, with care taken not to damage the retinal blood supply. To identify RGCs in the ganglion cell layer (GCL), we performed retrograde labeling by placing a small piece of gelfoam soaked with 2% aqueous Fluorogold (FG; Fluorochrome, Englewood, CO) containing 1% dimethylsulfoxide (DMSO) at the optic stump after optic nerve axotomy. Fifteen minutes before optic nerve surgery, 1 μg of GDNF, NRTN, or ARTN (Peprotech, Rocky Hill, NJ) in phosphate-buffered saline (PBS; 3 μl) containing 0.1% bovine serum albumin (BSA) was injected intravitreally by puncturing the eyeball at the cornea–sclera junction with a 32-G needle on a Hamilton syringe. Animals were excluded if the lens was injured during the course of intraocular injection.

For the in vivo experiment for axon regeneration, the optic nerve was crushed as previously described (Kurimoto et al. 2006, 2010). The animal was anesthetized with 7% chloral hydrate solution (400 mg/kg). After skin incision, the left optic nerve was exposed and mechanically crushed with jewelry forceps (Dumont No. 545; World Precision Instruments, Tokyo, Japan) for 10 sec, 2 mm behind the eye. We verified, with a direct ophthalmoscope, that the integrity of the retinal blood supply was not damaged. To investigate the effect of GDNF, NRTN, and ARTN on axon regeneration, all reagents were injected into the vitreous with a glass micropipette through a hole made by a 27-G needle on days 0, 1, 4, and 7.

Twelve days after the optic nerve was crushed, the operated animals were anesthetized with a 7% chloral hydrate solution, and 3 μl 1% cholera toxin B subunit solution (CTB; List Biological Laboratories, Campbell, CA) was intravitreally injected. Two days after the CTB application, the animals were transcardially perfused with 4% paraformaldehyde (PFA) in phosphate buffer. The optic nerve was dissected and immersed in 30% sucrose for cryoprotection, and then it was sectioned longitudinally at a thickness of 16 μm. After being blocked, the sections were incubated by 1:4,000 goat anti-CTB antibody (List Biological Laboratories) and in 1:200 biotinylated rabbit anti-goat IgG antibody (Vector Laboratories, Burlingame, CA) for 2 hr at room temperature (RT), followed by 1:400 Alexa 488-conjugated streptavidin (Molecular Probes, Eugene, OR). The sections were then mounted with antifade reagent (Molecular Probes), and axons were counted as previously described (Kurimoto et al., 2006). Under fluorescent microscopy (Optishot; Leica, California), CTB-labeled axons were directly counted at each grid line 250, 500, or 1,000 μm from the distal end of the crush site. The mean number of axons at each distance was calculated from seven to 10 sections per animal.

### RNA Extraction and Quantitative Reverse Transcription-Polymerase Chain Reaction

RNA extraction and real-time reverse transcription-polymerase chain reaction (RT-PCR) were performed as previously described (Nakazawa et al., 2000), with minor modification. Retinas were directly lysed in Qiagen (Hilden, Germany) RNeasy RLT lysis buffer. Subsequent RNA extraction was performed with the RNeasy microkit (Qiagen) according to the manufacturer's instructions. Total RNA (200 ng) was reverse transcribed by using a SuperScript III first strand synthesis kit (Life Technologies, Frederick, MD) to synthesize cDNA. First-strand cDNA was amplified by using the Expand Long Template PCR system (Boehringer Mannheim, Indianapolis, IN), with PCR primer sets for GFRα1 5′-TGG CAGCCAGCCCCTCCAGTCCA-3′ and 5′-TTGGGTG AAACTGCTTCTCAACG-3′, GFRα2 5′-TCTCCCAAA GGCCCCTCACTCCCA-3′ and 5′-ATGTGTGTATGCGTG TGTTTCCA-3′, GFRα3 5′-GAGCATGCTCAAACCAGACT CCGA-3′ and 5′-TGTGGAAACGCATTTTAGCCGCAA-3′, and Ret 5′-TGGGCCAGTATCTCTATGGCGTCT-3′. RT-PCR of 18S ribosomal RNA (5′-CATGCATGTCTAAGTACG CACGG-3′ and 5′-CGGCGACTACCATCGAAAGTTGA-3′) was used as an internal control for the reactions. PCR amplification was performed by using the GeneAmp PCR System 2400 (Perkin Elmer/Applied Biosystems, Waltham, MA) for the number of cycles indicated as GFRα1 (24 cycles), GFRα2 (24 cycles), GFRα3 (28 cycles), Ret (24 cycles), and 18S (10 cycles) with denaturation at 96°C for 30 sec, annealing at 60°C for 30 sec, and extension at 72°C for 90 sec, followed by extension at 72°C for 7 min. PCR products were evaluated by agarose gel electrophoresis followed by staining with ethidium bromide and sequencing. The gel was photographed by using short wave-length UV, and the fluorescent intensity of the product bands was determined by

densitometry. To ensure that measurements were in a linear range, the intensity of the PCR product bands of several cycles was measured by densitometry and plotted to determine its linear range of amplification (data not shown). The data presented were all in the linear range.

For the real-time quantitative PCR, first-strand cDNA was amplified with a 7500 fast real-time PCR system (Applied Biosystems, Foster City, CA) with Taqman probe sets (Life Technologies) for GFRα1 (Rn01444617_m1), GFRα2 (Rn00562583_m1), GFRα3 (Rn01760829_m1), Ret (Rn01463098_m1), and glyceraldehyde-3-phosphate dehydrogenase (GAPDH; Rn01462662_g1). Relative gene expression levels were calculated by using the ΔΔCt method.

### Counting FG-labeled RGCs in Retinal Flat Mounts

Preparation of whole-mounted retina was as previously described (Nakazawa et al., 2002a,b). Rats were sacrificed by an overdose of Nembutal 10 days after optic nerve transection. Retinas were dissected, fixed in 4% PFA. and flat mounted onto glass slides. RGC densities were determined by counting FG-labeled RGCs in 12 distinct areas, each measuring $7.29 \times 10^{-2}$ mm$^2$ (three areas per quadrant at 1/6, 3/6, and 5/6 of the distance from the optic nerve head to the periphery along a retinal radius). The density of FG RGCs was defined as the average value of the 12 fields counted and analyzed statistically, as previously described (Nakazawa et al., 2002a,b). The counting of FG-labeled RGCs was conducted under microscopy in a masked fashion by two independent investigators.

### Immunoblot and Immunohistochemistry

Three days after treatment with or without axotomy, the retinas were isolated and placed into a sampling buffer as HBS (pH 7.4) containing 1% protease inhibitor cocktail (Sigma-Aldrich, St. Louis, MO) and homogenized in lysis buffer as HBST (0.5% Triton X-100, pH 7.4) containing 1% protease inhibitor cocktail. Cell lysates were clarified by centrifugation at 15,000*g* at 4°C for 20 min. Each cell lysate was collected into a new tube, and quantity of protein concentration was determined by using a BCA kit (ThermoFisher Scientific, Rockford, IL). For each sample, 10 μg total protein was applied per lane, separated with sodium dodecyl sulfate-polyacrylamide gel electrophoresis, and electroblotted onto a polyvinylidene fluoride (PVDF) membrane (Millipore, Bedford, MA). After nonspecific binding had been blocked with 8% Block Ace (Yukijirushi, Sapporo, Japan), the membranes were incubated at 4°C overnight with a rabbit polyclonal antibody against GFRα3 (1:1,000, ab-8028; Abcam, Cambridge, MA) and β-actin (1:5,000, A5316; Sigma-Aldrich). The membranes were then incubated with a horseradish peroxidase-conjugated anti-rabbit or anti-mouse immunoglobulin secondary antibody for 1 hr. The signals were visualized with chemiluminescence (ECL prime blotting analysis system; GE Healthcare, Tokyo, Japan), measured in Image Lab statistical software (Bio-Rad, Hercules, CA), and normalized to β-actin.

Immunohistochemistry was performed as previously described (Nakazawa et al., 2002a,b). Briefly, surgically removed retinas were fixed with 4% PFA at 4°C overnight and then cryoprotected with PBS, 0.1 M phosphate buffer (pH 7.4), and 0.15 M NaCl containing 20% sucrose. Cryosections (10 μm) were mounted on slides and incubated with blocking buffer (10% goat serum, 0.5% gelatin, 3% BSA, and 0.2% Tween-20 in PBS) for 1 hr. Then the sections were incubated with blocking buffer and a primary antibody made in rabbit against GFRα3 (AB5400; Chemicon, Temecula, CA). Normal serum (Dako, Osaka, Japan) was used as a negative control. The sections were then incubated with Alexa TM 488-labeled secondary antibody (1:200 in blocking buffer; Molecular Probes) for 1 hr. Slides were washed three times with PBS containing 0.2% Tween-20 and mounted with Vectashield mounting media with 4′,6-diamidino-2 phenylindole (DAPI; Vector Laboratories). Photographs of the retina were taken routinely at an area 1 mm from the center of the optic nerve with a fluorescent microscope (Qfluoro system; Leica Microsystems, Wetzlar, Germany) with a UV filter (DAPI) and an FITC filter (immunostaining).

For double staining with GFRα3 and Brn3a, retinal sections were sliced (12 μm thick) with a cryostat and collected on MES-coated slides (Matsunami, Osaka, Japan). For the immunohistochemistry procedure, sections were blocked with 10% normal serum and 1% Triton X-100 in PBS for 1 hr at RT and then reacted with primary antibodies rabbit anti-GFRα3 (1:50, ab8028; Abcam) and mouse anti-Brn3a (1:200, sc-8429; Santa Cruz Biotechnology, Santa Cruz, CA) overnight at 4°C. After being washed in PBS, the sections were incubated with Alexa TM 488 (GFRα3)- or 568 (Brn3a)-labeled secondary antibodies for 1 hr at RT and mounted on Vectashield mounting media with DAPI. The sections were analyzed with a Leica TCS SP2 laser scanning spectral confocal microscope.

### Adult Rat Retinal Primary Cultures

Adult primary retinal cultures were prepared as previously described (Yin et al., 2006; Nakazawa et al., 2007). Cells from two retinas were resuspended in 1 ml Neurobasal A medium (Invitrogen, Carlsbad, CA) containing B27 supplement (Invitrogen) with antioxidants for axonal growth analysis (NBA/B27AO$^+$) or without antioxidants for cell survival assay (NBA/B27AO$^-$), and cells were counted by using a hemocytometer after incubation with the same volume of 0.4% Trypan blue solution (Sigma). Cell density was adjusted to $4 \times 10^5$ cells/ml with culture medium, and 100 μl cell suspension was seeded into each well of an eight-well chamber (Nunc; $4 \times 10^4$ cells per well). Ten minutes after seeding the cells, the total volume in each well was brought up to 400 μl by adding 300 μl of culture medium containing 1 μg/ml insulin, 2 mM L-glutamate, and 12 μg/ml gentamycin. One hour later, GDNF, NRTN, and ARTN at specified concentrations were added to the culture medium, and incubation continued in a 5% $CO_2$ atmosphere at 37°C for 24 hr for cell survival assay or for 72 hr for axonal growth analysis. Cells were then gently washed with PBS and fixed with 4% PFA for 10 min at RT. To assess the viability of RGCs, we performed immunocytochemistry with mouse anti-β3-tubulin antibody, an RGC marker (Nakazawa et al., 2007). Briefly, cells were permeabilized with 0.1% Triton X-100 in PBS for 5 min and blocked by blocking buffer for 30 min at RT. Cells were then incubated with a monoclonal anti-β3-tubulin antibody (1:150 dilution; Sigma) at RT for 2 hr, rinsed with PBS (3 × 5 min), incubated with goat anti-mouse

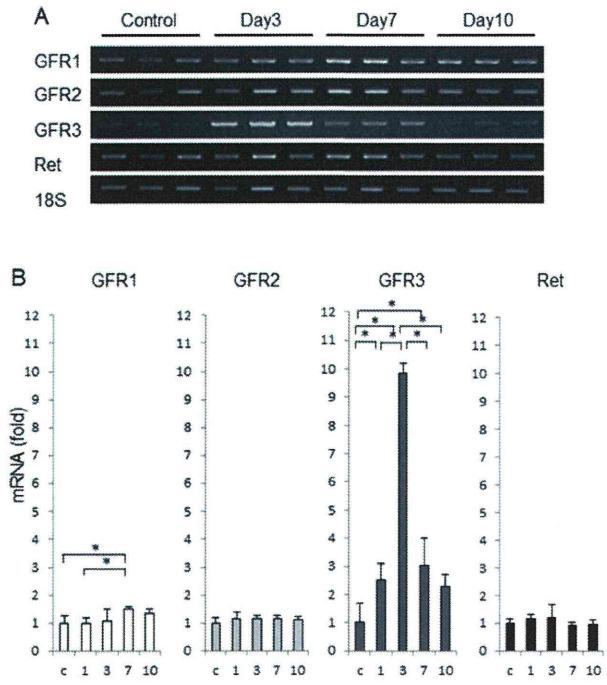


Fig. 1. Changes in expression of mRNA for GDNF-related genes and their receptors on days 3, 7, and 10 after axotomy. **A:** Representative gel images of RT-PCR products. **B:** Quantitative data of real time RT-PCR on days 1, 3, 7, and 10 after axotomy; c, control. $*P < 0.05$.

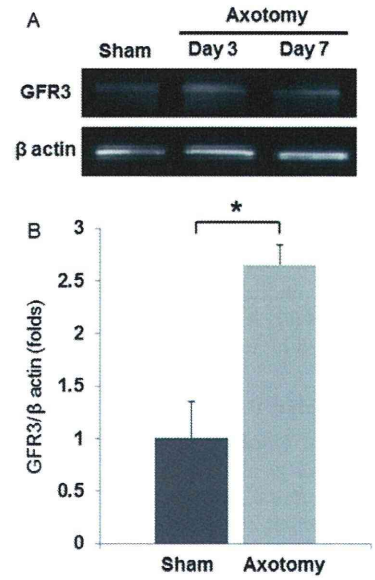


Fig. 2. Changes in expression of protein for GFRα3 on days 3 and 7 after axotomy. **A:** Representative images of immunoblot of sham, day 3, and day7 after axotomy. Upper panel, GFRα3; lower panel, β-actin. **B:** Quantitative data of immune blot of GFRα3/β-actin 3 days after axotomy. $*P < 0.05$.

secondary antibody (1:200, Alexa Fluor-488; Molecular Probes) at RT for 1 hr, and rinsed again with PBS (3 × 5 min). Eight-well chamber slides were mounted with Vectashield mounting medium with DAPI. Controls were stained by omitting the primary antibody. Samples were arranged in a pseudorandomized manner on the plates so that the investigator would not be aware of their identity when quantifying β3-tubulin-positive RGCs. The number of β3-tubulin-positive RGCs was counted in the following manner. Ten random fields per well were captured with a fluorescent microscope (×20 objective) equipped with an imaging system, and the β3-tubulin-positive RGCs were counted in ImageJ. RGCs with axons greater than two RGC diameters in length were defined as RGCs with neurite outgrowths. Values are the mean ± SEM of four replicate wells. Experiments were repeated at least three times. For inhibitor studies, we added U0126, LY294002, SB203829, or JNK2 (Merck-Millipore, Billerica, MA) to the culture medium, and 30 min later ARTN was administered at a final concentration of 1, 10, or 100 ng/ml.

### Statistical Analysis

The data from the experimental and control groups were analyzed with ANOVA followed by Scheffé post hoc test in StatView 4.11J software (Abacus Concepts, Berkeley, CA). Statistical analysis for optic nerve regeneration in vivo was performed with the Tukey honest significant difference test. All values were expressed as mean ± standard deviation. $P < 0.05$ was considered statistically significant.

## RESULTS

### RNA Expression of GFR-Related Genes After Optic Nerve Axotomy

To investigate expressional changes of GFR-related genes after optic nerve axotomy, we performed real-time RT-PCR with several primer sets including GFR-related genes and their coreceptor, Ret. We harvested neural retinas at various time points (control and days 1, 3, 7, and 10) after optic nerve axotomy. Real-time PCR data showed that the expression of GFRα3 increased greater than tenfold 3 days after axotomy ($P < 0.01$; Fig. 1), whereas other members of the GFR family (GFRα1 and GFRα2) were unchanged on day 3. On day 7 after axotomy, the expression of GFRα1 was significantly increased (1.5-fold, $P < 0.05$), and induction of GFRα3 expression was less than on day 3 but still significantly greater than baseline (threefold; $P < 0.05$). On day 10 after axotomy, the expression of all GFR-related genes had returned to control levels. The expression of Ret remained constant during this time period (Fig. 1). We next investigated the protein expression on days 3 and 7 after axotomy. GFRα3 protein had increased significantly by day 3 after axotomy compared with the sham-treated eyes (2.65 ± 0.2-fold, $P < 0.05$; Fig. 2). Immunoblot and immunohistochemistry (IHC) showed that immunoreactivity for GFRα3 antibodies was active in the GCL and inner nuclear layer (INL) and slightly active in the inner plexiform layer (IPL; Fig. 3A). On day 3 after axotomy, immunoreactivity for GFRα3 antibodies was significant

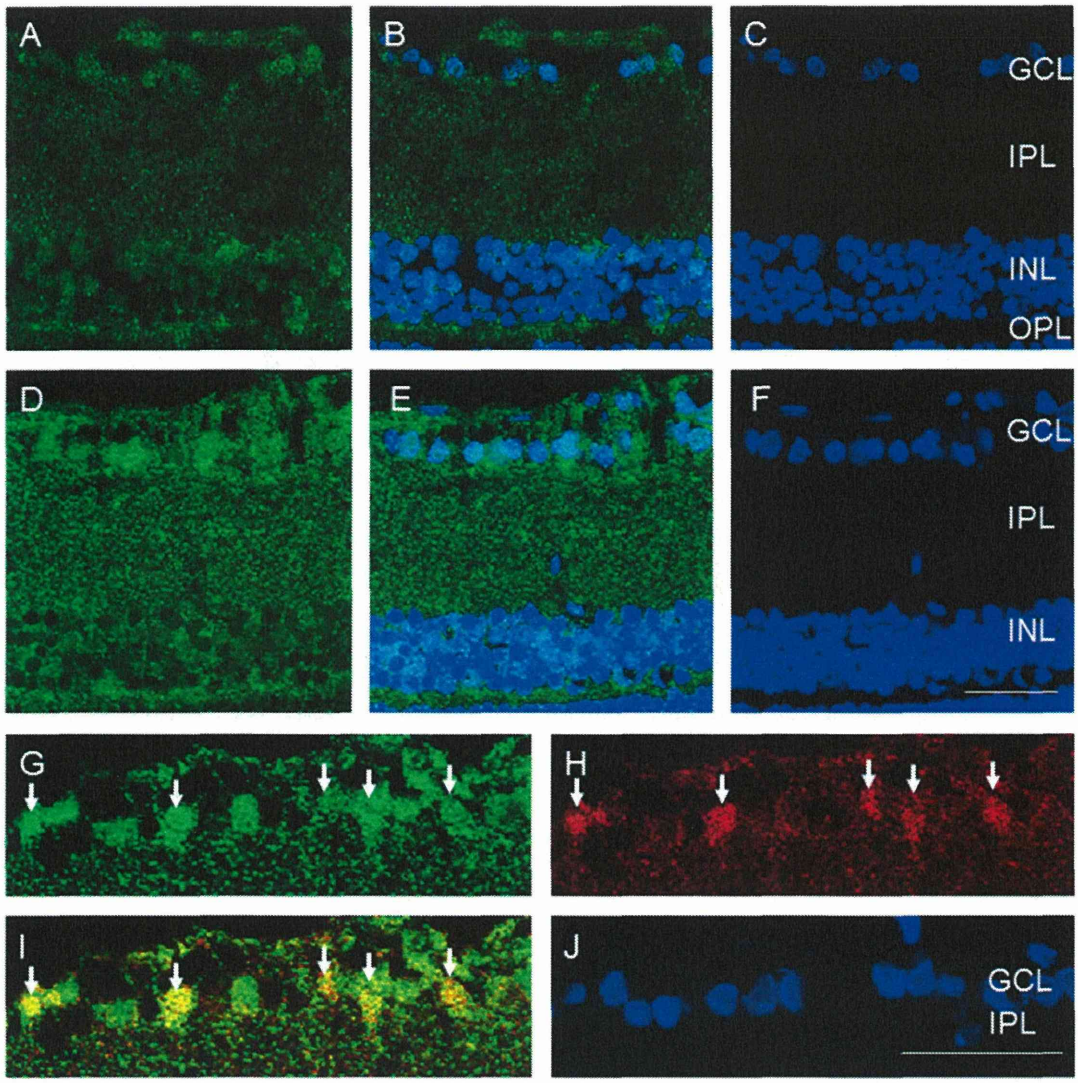


Fig. 3. Representative confocal microscopy photographs of immunohistochemical staining in adult rat retinas with GFRα3 antibodies with or without axotomy. **A–C:** Control retina. **D–J:** Day 3 after axotomy. A,D,G: Immunoreactivity of GFRα3 antibody. B,E,I: Merged images. C,F,J: DAPI nuclear staining. H: Immunoreactivity of Brn3a, an RGC marker. The arrows show RGCs with colocalized GFRα3 and Brn3a. GCL, ganglion cell layer; IPL, inner plexiform layer; INL, inner nuclear layer; OPL, outer plexiform layer. Scale bars = 50 μm.

in the inner retina, including the GCL, IPL, and INL (Fig. 3D). GFRα3 protein was colocalized in the Brn3a-positive RGCs (Fig. 3G–I). These data suggest that GFRα3 is dramatically upregulated following axonal injury at a critical point for RGC survival.

### GFRα3 Expression During Retinal Development

Axonal damage can activate neurons' intrinsic axonal growth program, which partially recapitulates an earlier developmental state of neurons (Wang et al., 2007). This possibility prompted us to investigate the expression of GFRα3 and other GFRs during retinal development. Real time RT-PCR showed that the pattern of GFR-family gene expression changed dramatically over the course of retinal development. At embryonic day 14 (E14), the neuroblastic layer (NBL) had just formed (Nakazawa et al., 2000, 2002a), and the expression of GFRα3 stood out among all GFR family members (Fig. 4). At E17, two cellular layers could be distinguished in

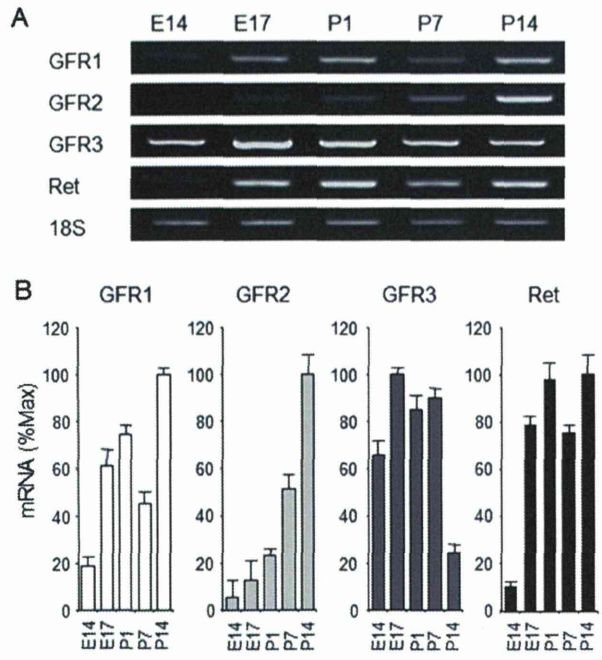


Fig. 4. Developmental profiles of mRNA expression for GDNF-related genes. **A:** Representative gel images of RT-PCR products. **B:** Quantitative data of RT-PCR at E14, E17, P1, P7, and P14. E, embryonic day; P, postnatal day.

the NBL and GFRα1 and GFRα3 were expressed, but GFRα2 expression remained weak. This pattern remained substantially unchanged at postnatal day 1 (P1), when the GCL is separated from the NBL. At P7, the outer plexiform layer (OPL) has formed, and the INL and outer nuclear layer (ONL) can be distinguished. Here, GFRα1 expression decreased and GFRα3 expression remained high, whereas GFRα2 expression began to increase. At P14, retinal layer structure is very similar to adult retinal layer structure, and expression of GFRα1 and GFRα2 increased, whereas the expression of GFRα3 decreased. The expression of Ret was detectable from E17, and the level of Ret mRNA was constant through P14. These data suggest that the expression of GFRα3 is highest in the immature retina and then declines, whereas GFRα1 and GFRα2 are highly expressed in the mature retina. The expression of GFRα3 appears earlier than that of Ret, at E14.

To investigate the distribution of GFRα3 protein in the developing retina further, we performed IHC by using an anti-GFRα3 antibody. At P1, GFRα3 immunoreactivity was detected in the entire retina but was stronger in the cells of the GCL than in the NBL (Fig. 5). At P7, the expression of GFRα3 was strongest in the GCL, IPL, and inner margin of INL. At P14, GFRα3 was detected in the GCL, IPL, inner margin of INL, OPL, and outer segment. These data indicate that, during development, GFRα3 is expressed at its highest levels in the inner retina, including the GCL, IPL, and INL.

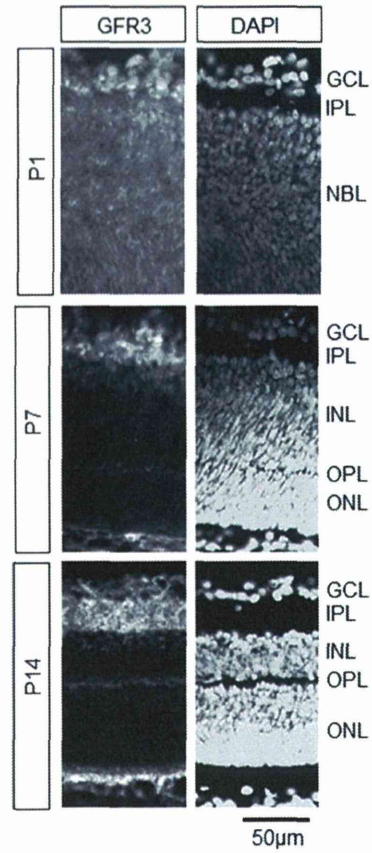


Fig. 5. Immunohistochemical staining with a GFRα3 antibody in the developing retina. Upper panels show results at P1, middle panels at P7, and lower panels at P14 after birth. Left images are IHC for GFRα3 and right images are DAPI nuclear staining. P, postnatal day; GCL, ganglion cell layer; IPL, inner plexiform layer; NBL, neuroblastic layer; INL, inner nuclear layer; OPL, outer plexiform layer; ONL, outer nuclear layer.

## Neuroprotective Effect of GFRα3

Next, we investigated the neuroprotective effect of GDNF-family proteins on RGCs in dissociated adult rat primary cultures. We found that GDNF, NRTN, and ARTN all had a neuroprotective effect on adult RGCs at a concentration of more than 10 ng/ml (Fig. 6A–E). To examine the signaling pathway, we treated cells with several pathway inhibitors (U0126 as an MEK inhibitor, LY294002 as a PI3K inhibitor, SB203580 to inhibit p38, and JNK2 to inhibit JNK) in the presence or absence of ARTN (Fig. 6F). Baselines differed with kinase inhibitors in these cultures. Specifically, inhibition of the p38 and JNK pathways had a significant neuroprotective effect on dissociated RGCs in vitro. The quantitative count on the surviving RGCs suggested that the neuroprotective effect of ARTN was suppressed by MAPK and PI3K inhibitors but not by inhibitors of p38 and JNK, suggesting that the neuroprotective effect on cultured RGCs occurs through the MAPK and PI3K signaling pathways.

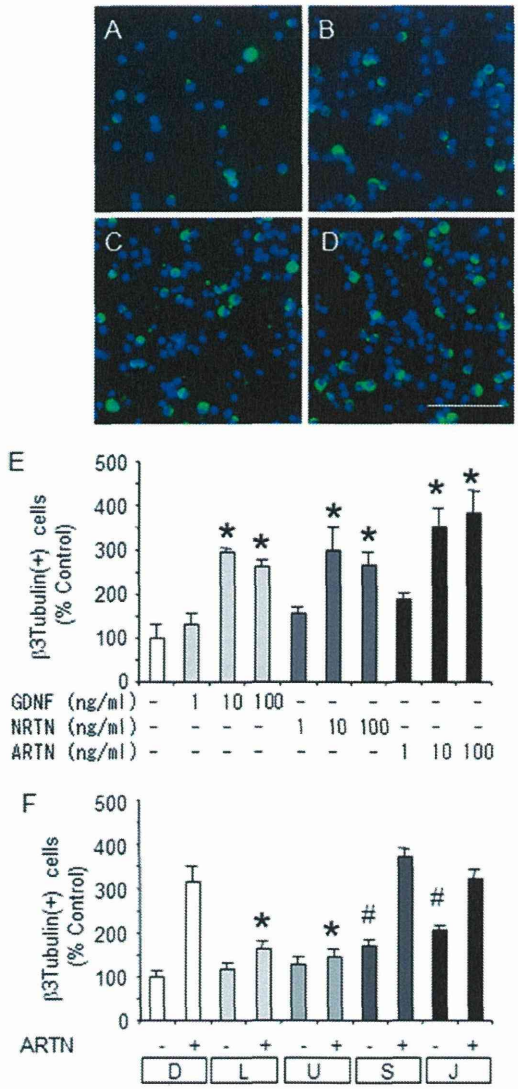


Fig. 6. Representative images of surviving β3-tubulin-positive RGCs following stimulation with GDNF-related proteins in vitro. **A:** PBS. **B:** GDNF. **C:** NTRN. D: ARTN. **E:** Quantitative data of β3-tubulin-positive RGCs with different doses of GDNF-related proteins after 24 hr in vitro. $*P < 0.05$ compared with control without trophic factors. **F:** Quantitative data of β3-tubulin-positive RGCs following treatment with ARTN combined with signaling inhibitors after 24 hr in vitro. D, DMSO; L, LY294002; U, U0126; S, SB203580; J, JNK inhibitor II. $*P < 0.05$ compared with ARTN with DMSO; $^{\#}P < 0.05$ compared with ARTN$^-$ condition with DMSO. Scale bar = 50 μm.

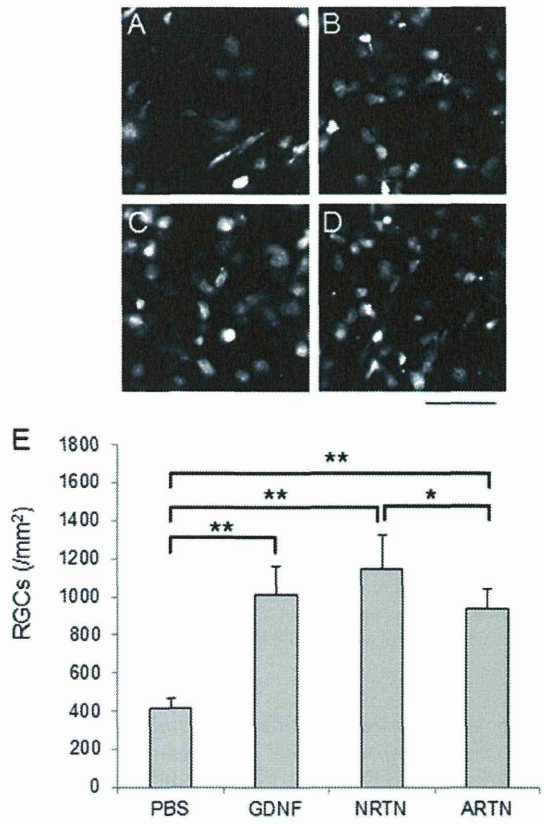


Fig. 7. Representative photographs of FG-labeled RGCs on day 10 after axotomy. **A:** Axotomy with intravitreal administration of PBS. B: GDNF. **C:** NRTN. **D:** ARTN. **E:** Quantitative data of surviving FG-positive RGCs 10 days after axotomy following treatment with PBS, GDNF, NTRN, and ARTN. $*P < 0.05$, $**P < 0.01$. Scale bar = 100 μm.

To investigate whether GDNF family members have a neuroprotective effect on RGCs, we examined the effects of GDNF, NRTN, and ARTN on the survival of axotomized RGCs in vivo. Ten days after optic nerve damage and intravitreal injection of GDNF family members (1 μg per eye), the retina was harvested, and the density of FG-positive RGCs was counted. The density of FG-labeled RGCs was found to be $415 \pm 50$ cells/mm$^2$ after injecting PBS ($n = 10$), $1{,}013 \pm 150$ with GDNF ($n = 10$; $P < 0.0001$), $1{,}143 \pm 150$ with NRTN ($n = 10$, $P < 0.0001$), and $935 \pm 107$ with ARTN ($n = 10$, $P = 0.001$; Fig. 7). There was a significant difference between NRTN and ARTN ($P = 0.045$). These data suggest that GDNF family proteins have a neuroprotective effect on axotomized RGCs.

## Effect of Axonal Regeneration in Vivo and in Vitro

At E14, developing RGCs extend their axons toward the brain, and expression of GFRα3 is much higher than GFRα1 and GFRα2 at this time point. This developmental profile of GFRα3 led us to investigate the effect of ARTN on axonal growth after injury in adult animals. No significant differences were found in surviving RGCs after 72 hr in vitro with antioxidants and treatment with PBS ($40.3 \pm 6.6$ cells per field; CPF), GDNF ($52.4 \pm 9.4$ CPF), NRTN ($58.3 \pm 7.9$ CPF), or ARTN ($54.7 \pm 12.0$ CPF). Therefore, we showed the percentage

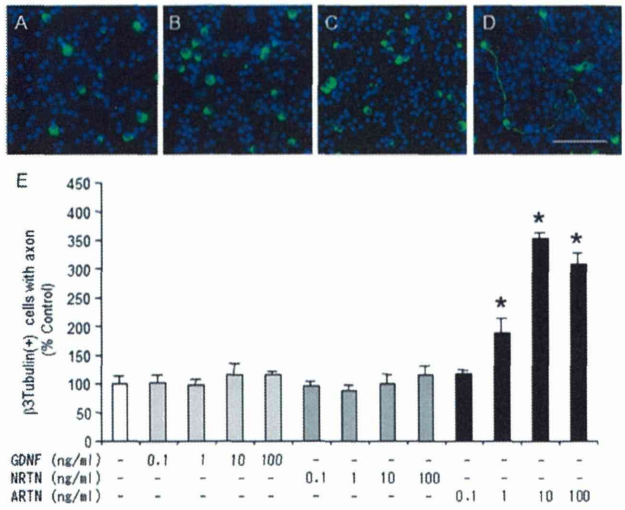


Fig. 8. Images of β3-tubulin-positive RGCs with axonal growth following the stimulation of GDNF-related proteins in vitro. **A:** PBS. **B:** GDNF. **C:** NTRN. **D:** ARTN. **E:** Quantitative data of axonal growth in β3-tubulin-positive RGCs after 72 hr in vitro. $*P < 0.05$ compared with control without GDNF family protein. Scale bar = 50 μm.

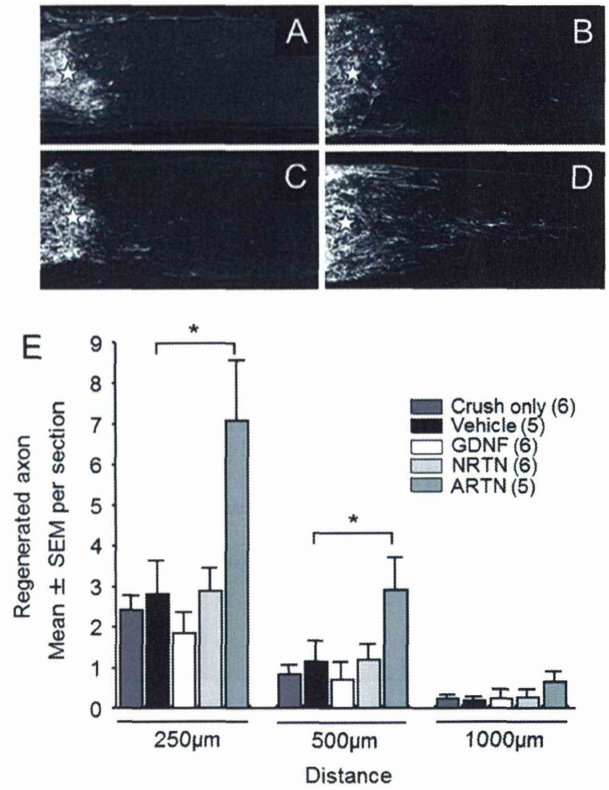


Fig. 9. Representative photographs of axonal regeneration following multiple injections of GDNF-related proteins in vivo. Stars indicate the crush site. **A:** PBS. **B:** GDNF. **C:** NTRN. **D:** ARTN. **E:** Quantitative data of β3-tubulin-positive RGCs with axonal growth at distances of 250, 500, and 1,000 μm on day 21 after optic nerve crush. $*P < 0.05$ compared with vehicle control in the same points.

in order to compare the different conditions. In culture, ARTN had a strong effect on axon outgrowth after 72 hr, whereas GDNF and NRTN did not (Fig. 8). We also detected similar effects of ARTN on axonal regeneration in vivo with multiple administrations (Fig. 9). These results indicate that, among GDNF family members, ARTN and its receptor GFRα3 have a unique effect on axonal growth of RGCs.

## DISCUSSION

This study demonstrates that optic nerve injury induces the upregulation of GFRα3 within 3 days, a critical time point for determining the fate of injured RGCs. To gain insight into the role of GFRα3 after axotomy, we investigated its expression during retinal development and found that, among GDNF family members, the expression of GFRα3 was particularly high throughout embryonic development and in the early postnatal period, then gradually decreased at later stages of maturation. Profiles of GFRα1 and GFRα2 expression were very different from that of GFRα3, suggesting substantial differences in the roles of different GFR family members during development. To examine the role of GFRα3 further, we assessed the effects of ARTN on RGC survival and axon regeneration both in vivo and in vitro. All of the GDNF family members (GDNF, NRTN, and ARTN) had neuroprotective effects on axotomized RGCs. Investigation of intracellular signaling pathways suggested that the neuroprotective effect of ARTN was through the MAPK and PI3K signaling pathways. However, among GDNF family members, ARTN alone stimulated the regrowth of RGC axons both in vivo and in vitro. These findings suggest that the ARTN–GFRα3 pathway contributes to the survival and axonal growth of axotomized RGCs in a way that is unique among GDNF family members.

The present study indicates that both GDNF and NRTN had a neuroprotective effect on axotomized RGCs. This is in agreement with the findings of previous studies that used RGC injury models (Koeberle and Ball, 2002; Ozden and Isenmann, 2004; Ward et al., 2007). Here, we also report for the first time that ARTN had a neuroprotective effect on axotomized RGCs. The neuroprotective effect of NRTN was strongest among GDNF family members, whereas the neuroprotective effect of ARTN was weaker than that of the other members. One possibility is that the roles of ARTN and GFRα3 might differ in RGC survival and axonal growth.

Seventy-two hours after axotomy, the expression of GFRα3, the embryonically dominant form of the GFR family, was significantly upregulated. Previously, we had shown that RB3, a tubulin disassembly factor, is also upregulated in the GCL and peaks at 3 days after optic nerve axotomy (Nakazawa et al., 2005a). Tubulin remodeling is a critical step for axonal growth. Furthermore,